SURFACE MAGNETIC FIELDS AND UV RADIANCE OF THE QUIET SUN

A. Pauluhn[(1)] **and S. K. Solanki**[(2)]

[(1)]*International Space Science Institute, Bern, Switzerland, e-mail: pauluhn@issi.unibe.ch*
[(2)]*Max-Planck-Institut für Aeronomie, Katlenburg-Lindau, Germany, e-mail: solanki@linmpi.mpg.de*

ABSTRACT

In order to investigate the correspondence between the quiet-Sun UV radiance and changes in the magnetic network during the solar cycle, we study the quiet-Sun variability with the two EUV instruments CDS (Coronal Diagnostic Spectrometer) and SUMER (Solar Ultraviolet Measurements of Emitted Radiation) and the MDI (Michelson Doppler Imager) magnetograph on SOHO. Using a monthly data set of co-spatial and co-temporal observations of quiet-Sun areas near disk centre we follow the evolution of the quiet Sun over four years from solar minimum to solar maximum conditions. Although the magnetic flux of the quiet network increases by a rather low percentage over the solar cycle, its variation is well correlated with the radiance change in the He I 584 Å line. We test our data set of quiet-Sun measurements for a pixelwise relation between magnetic flux density and radiance.

1. INTRODUCTION

The fact that the solar irradiance at UV wavelengths exhibits significant variations over the solar cycle has been known for a considerable time, see e.g., [1] or [2]. In general, changes in the magnetic flux at the solar surface and its concentration into dark sunspots and bright faculae or plages are thought to be the drivers of the irradiance variations, although there have also been calls for alternatives. The question of the source of EUV variability has become of renewed interest since the discovery that the brightness of EUV lines recorded in selected quiet-Sun regions by SUMER has increased from solar activity minimum to maximum [3]. There are different possible explanations for this result. Either the magnetic flux has increased in these "quiet" regions with time, or they have changed in some other fundamental way.

Here we study, using MDI magnetograms, whether the former explanation is correct. This is motivated by the correspondence of magnetic field strength and radiative intensity which is evident from inspection of spectroheliograms and magnetograms and has been described in several studies, e.g., by [4, 5, 6, 7, 8, 9, 10]. The aim of this work is on the one hand to compare the long term behaviour of the magnetic field measured by MDI with the long term behaviour of the EUV radiances measured with SUMER and CDS, and on the other hand to investigate with our data sets the relation between radiative and magnetic field which generally is neither simple nor linear [11, 1].

After a description of the data reduction (Sect. 2), we outline the use of the magnetogram data to follow the Sun's activity cycle and identify co-spatial and co-temporal measurements of the three instruments and investigate trends in the data sets (Sect. 3). Using these co-located images, we look for a relation between radiative and magnetic flux for the particular case of the He I 584 Å line (Sect. 4). A summary of the results and conclusions is given in Sect. 5.

2. DATA DESCRIPTION

2.1. The CDS and SUMER data

The data used in this work, spectral profiles of He I 584 Å, were obtained during Joint Observation Programme (JOP) Intercal_01, during which CDS [12] and SUMER [13] pointed simultaneously at the same parts of a quiet region near solar disk centre.

The effective pixel size of CDS is 4″ in the horizontal (cross slit) direction and 1.68″ vertical (along slit), although the actual spatial resolution is lower [14, 15]. The CDS instrument scanned an area of 60″×240″ during this JOP. The CDS data were corrected for burn-in and the flatfield. Prior to November 1996 the monthly SUMER quiet-Sun raster scans registered an area of 60″×300″ with 1″ vertical resolution and a step size of 0.76″ in east-west direction. After November 1996, the scans were rendered by the drift of the solar surface across the slit due to solar rotation. Thus the area sampled was 3.5″×300″. The SUMER data were corrected for the flatfield, the geometric distortion, and for detector electronics effects such as dead-time and local-gain depression. After the instrumental corrections and the radiometric calibration, the solar radiances were determined by integration over the line profiles, which were derived by least-squares fits of single Gaussian functions and a linear background. The background (continuum) was subtracted prior to integration. For more information on the data and the reduction we refer to [16].

Proc. 'SOLMAG: Magnetic Coupling of the Solar Atmosphere Euroconference and IAU Colloquium 188'
Santorini, Greece, 11-15 June 2002 (ESA SP-505, October 2002)

2.2. The MDI data

The MDI instrument [17] measures the photospheric longitudinal magnetic field. For our studies we selected the full disk 5-minute integrated magnetograms that have a spatial binning of 2″ per pixel. These images are taken every 96 minutes, 15 per day, and have a noise level of σ_{ns} = 9 G (A. Kosovichev, personal communication, 2001). To match the available CDS and SUMER data, the magnetograms closest in time to the EUV instruments' data were selected and the co-spatial areas were identified after compensating for solar rotation. From the 1024 px × 1024 px full disk MDI image we extracted a box of 200″× 400″ (100 px × 200 px) centered around the CDS image centre coordinates. A first approximation of the absolute magnetic flux density was computed as the absolute values of the MDI data in the box. Via two-dimensional cross-correlation the areas co-spatial to the CDS and SUMER images were determined where possible.

3. VARIATION OVER THE SOLAR CYCLE

Fig. 1 shows the mean value per image of the MDI measured line-of-sight flux densities for the full disk images as well as for the quiet areas comparable to the SUMER and CDS images. In the full Sun images, the mean value

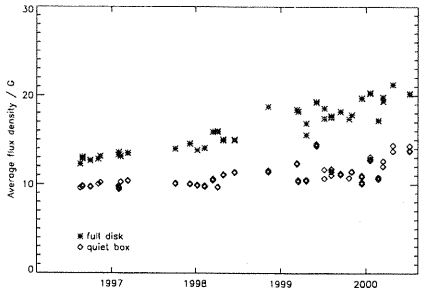

Figure 1. Mean of the magnetic flux density values in the MDI images of the full disk and the quiet area.

of the magnetic flux density increases by 30 % over the four years (mid 1996 to mid 2000), while in quiet areas the increase is roughly 10 %. It is shown by [18] that this increase is due to a rise in the network area where the magnetic signal exceeds 20 G. The area of the network measured over the full disk increased by a factor of 1.4 from solar minimum to maximum conditions. For the studied quiet areas this network area increased by a factor of 1.3.

Next we turn to the comparison between the data sets from the three instruments. For CDS the exact cospatial regions could be determined for all data sets, while for SUMER this was only possible in a minority of cases. For the remaining SUMER data sets (those without spatial scanning) only the averages over the entire images were compared. In Fig. 2 the time series of the image averages of these data sets are shown. For more information on the data see [18, 19] and references therein. A good correspondence is visible between the evolution of the EUV radiance and that of the magnetic flux. Already such a qualitative comparison suggests that the magnetic flux variations are responsible for the EUV flux variations. To obtain more quantitative estimates, we performed linear fits to the time series of the CDS data, the MDI data measured simultaneously with CDS, the SUMER data, and the MDI data measured simultaneously with SUMER. The trends are influenced by the selection of data points, e.g., by the choice of initial and end points for the fits, or by the distribution of the measurements. The uncertainties on the fractional increase over the time interval considered have been estimated from the two extreme curves resulting from the fit uncertainties in the two coefficients (constant a_0 and slope a_1), i.e., from the curves $(a_0 \pm \sigma_0) + t \cdot (a_1 \pm \sigma_1)$. Data points obviously contaminated with parts of active regions have been omitted from the fits which explains why the fit curves lie below the data around the activity maximum period in Fig 2. For the CDS time series we find an increase from May 1996 to May 2000 of (17 ± 10) %. The MDI data at the same dates and locations give an increase of (11 ± 5) %. For the co-temporal time series of SUMER and MDI, the relative increase amounts to (22 ± 25) % and (20 ± 15) %, respectively. The uncertainties of the linear fit parameters for the SUMER data are larger because the amount of SUMER measurements is smaller by nearly a factor of four. For the CDS and MDI data, the most pessimistic restrictions were those of omitting the first dates until March 1997 and those later than March 2000, giving small increases of 8 % (CDS) and 6 % (MDI) in four years.

In summary, a positive trend can be detected in all data sets, a conservative estimate of it would be a 10 % increase over four years. These fits have been made using approximately monthly measurements, with different temporal sampling during different periods, and as shown, the amount of the increase is not easily determined but strongly dependent on the chosen fit period. Nevertheless, our finding of an increase in the averaged magnetic flux of these areas supports the idea of a non-negligible contribution of the quiet Sun to the variability during the solar cycle.

4. CORRESPONDENCE OF RADIANCE AND MAGNETIC FIELD

A large number of investigations correlated the magnetic field and the Ca II H+K line flux, e.g., [20, 21, 22, 9, 11]. The relation between the 1600 Å continuum intensity and magnetic field has been studied by, e.g., [23, 24, 25, 26], and between the inner wing intensity of Mg I b lines and the magnetic field by, e.g., [27, 28], cf. also [29].

Skumanich et al. [9] found a linear relation between Ca II H+K line flux and magnetic flux density for the limited range between 25 G and 120 G. Schrijver et al. [11] extended their results to a nonlinear relationship between magnetic field and Ca II H+K line excess flux density, i.e., the flux density R minus a background R_0 and obtained a power law $R - R_0 = a \cdot B^b$, where B is the magnetogram signal and a is a calibration dependent factor. They determined the exponent b to be 0.6 ± 0.1. Harvey and White [30] found the exponent of

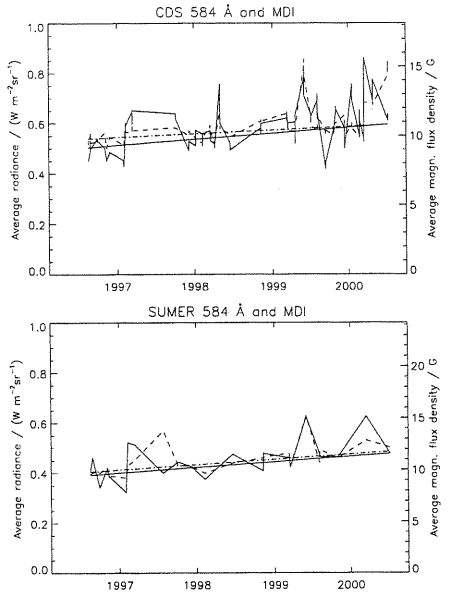

Figure 2. Time series of the average values of the CDS, SUMER and MDI images. The solid lines give the radiance data, and their linear fits, the dashed and dot-dashed lines give the MDI data and their corresponding fits. All shown fits give an increase of 11 % to 22 % within the four years from June 1996 to June 2000.

a general relationship to be 0.5, investigating full-disk magnetograms and Ca II K images for data sets in early 1992 (close to maximum solar activity of cycle 22) and mid 1993 (at lower solar activity). They conclude that the general relation is a square-root dependence, with the differences in the various structure classes (such as quiet parts, network, enhanced network, active regions) being due to different filling factors and divergence properties of the magnetic fields between these structures as described by a flux tube packing model [31, 32], the relation between R and B being general, and only the geometry of the flux tubes changing the details.

Our data set of more than four years of approximately co-spatial and co-temporal magnetograms and EUV images seems particularly suitable to test for the relation between magnetic flux density and EUV He I 584 Å radiance. We fitted a 2-parameter function $R = a \cdot B^b$, as well as a 3-parameter function $R = a \cdot B^b + c$, which admits a possible basal radiative flux that is uncorrelated with the magnetic field. The instrument resolution influences the fit parameters, a low resolution and a broad point-spread-function suggesting an instrumental rather than solar basal flux. In addition, the factor a and the constant c are dependent on the radiometric calibration of the EUV instruments. Several noise-cutoff values were tested for the fits, and in the following the MDI measurements < 10 G and the corresponding radiances have been neglected. The relations obtained for the full set of measurements were:

2-param.-fit:	3-param.-fit:
$R_{SUM}=0.12 \cdot B^{0.48}$	$R_{SUM}=0.13 \cdot B^{0.46} - 0.016$
$R_{CDS}=0.20 \cdot B^{0.46}$	$R_{CDS}=0.15 \cdot B^{0.50} + 0.09$

The uncertainties of the fit-coefficients varied mostly between 10 % and 30 %. However, while the uncertainty for the constant in the CDS-MDI fit amounts to 10 %, it is much larger in the SUMER-MDI fit, due to the small sample size. After scaling CDS and SUMER to the same average value, the coefficients agree to within a few percent. The large scatter in the corresponding plot (compare also Fig. 4) is partly a consequence of strongly deviating pixels in the range of small magnetic flux and high or intermediate EUV radiance as a consequence of mixed polarity fields that were simply averaged out in deriving the magnetic fluxes in the given resolution. Another possible source of high intensities at small B are shocks from acoustic waves [33]. Yet another possibility is the bigger spatial scale of the features in the EUV images than in the magnetograms which is responsible for the anomalous points. Thus regions of strong field are associated with a much larger region of strong emission, so that in a pixel-by-pixel comparison there are numerous points belonging to such EUV halos that do not correspond to a strong magnetograph signal, although obviously related to a nearby network element. That this effect plays an important role is suggested by the fact that the CDS data show a larger scatter than the SUMER data. A part of the scatter is probably also due to the large variability and transient events displayed by EUV lines [34, 35, 36]. Only time series with high temporal resolution can clarify how much scatter is introduced by this. An important source of uncertainty is the fact that the images are not exactly simultaneous, but can be offset by up to 48 minutes, and in few cases even more. Which of these sources of scatter is the dominant one cannot at present be judged.

For the time series of CDS and MDI images, two types of relations were found by visual inspection of the scatter plots, one group showing a tight pixelwise relationship between EUV radiance and magnetic field, and the other one showing two or more branches of the relation. The first group contained 53 % of the data, the second 34 %. 5 % of the data consisted of very low-field, noisy data and these, as well as 8 % of the data in which gaps dominate, have been omitted. Fig. 3

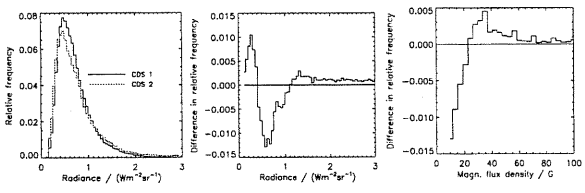

Figure 3. Left: Histograms of the CDS images from the two main groups. Middle: Difference of the two CDS histograms. Right: Difference of the two MDI histograms.

shows the two histograms of the radiances of the two groups, together with their difference and the difference for the corresponding MDI histograms. The radiance distributions of the second group have a steeper increase and an enhanced tail, meaning enhanced contrast.

The relations found for the first group were:

2-param.-fit:	3-param.-fit:
$R_{SUM}=0.15 \cdot B^{0.39}$	$R_{SUM} = 0.13 \cdot B^{0.42} + 0.04$
$R_{CDS}=0.25 \cdot B^{0.36}$	$R_{CDS} = 0.15 \cdot B^{0.44} + 0.15$

The relations found for the second group were:

2-param.-fit: $R_{SUM} = 0.09 \cdot B^{0.60}$ $R_{CDS} = 0.18 \cdot B^{0.52}$

3-param.-fit: $R_{SUM} = 0.14 \cdot B^{0.52} - 0.12$ $R_{CDS} = 0.15 \cdot B^{0.54} + 0.06$

The fit uncertainties range from less than 5 % to 20 % for most of the fits involving the CDS data.

Restricting oneself to the first group nearly eliminates the upper branch from the scatter plots, as can be seen in Fig. 4 (upper row), and the relation for the second group is dominated by that for the upper branch, see Fig. 4 (lower row).

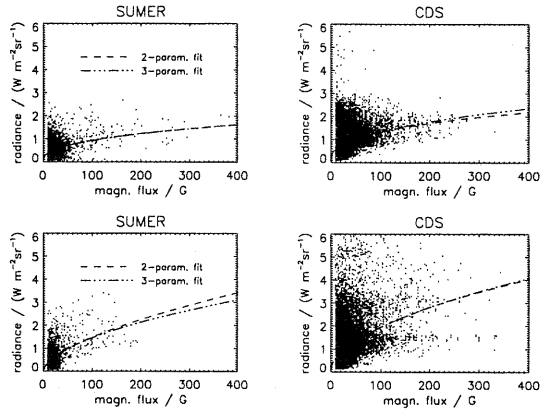

Figure 4. Scatter plots of the co-located SUMER and MDI and CDS and MDI images, respectively, where a good correlation has been found (upper plots), and where the fit runs through the upper branch or through the middle of the branches (lower plots).

Our study shows that also for chromospheric He I data at 584 Å a power-law relation between magnetic flux density and radiance can be established. Comparing our findings to earlier results obtained for other chromospheric spectral lines, a reasonably good agreement is achieved and confirms an approximately square-root power law. We do see some differences between regions with different activity levels (although the grouping is somewhat subjective). Thus, for the quiet network, the exponent lies around 0.44. Considering the fits for images where also more active network is present, the exponents increase slightly towards 0.5 to 0.6.

5. SUMMARY AND CONCLUSIONS

Four years of nearly monthly measurements of magnetic field and chromospheric EUV radiance of quiet regions near solar disk centre have been studied and compared, using data from SOHO's MDI magnetograph and the two EUV spectrometers CDS and SUMER. The time series begin in 1996 during the activity minimum between solar cycles 22 and 23 and accompany the rise of cycle 23 until mid 2000.

A small increase of around 10 % is recognized in the time series of the magnetic flux densities as well as in those of the radiances in He I 584 Å measured by CDS and SUMER. Thus, independent measurements of the two EUV instruments and the MDI magnetograph on SOHO seem to indicate that the so-called quiet Sun has a significant influence on solar variability.

Fits of power laws to the scatter plots suggest exponents of 0.42 to 0.58 for the magnetic flux density. However, our data sets mostly represent a very quiet part of the Sun, and the lower exponents represent the results for the quiet network. With progress of the solar cycle towards higher activity the network changes, and more active parts emerge in the network, so that on average the exponent increases. Our results agree well with the relations found by [11] who determined an exponent of 0.6 for Ca II H+K and [30] who analyzed Ca II K images and found a general square root relation between radiative and magnetic flux, with additional dependence on feature specific properties, like the flux tube density or filling factor.

REFERENCES

1. Lean, J., *ASP Conf. Ser.* 223, 109–116, 2001.
2. Solanki, S.K, et al., *IAU Symp.* 203, 66–77, 2001.
3. Schühle, U., et al., *Astron. Astrophys.* 354, L71–L74, 2000.
4. Babcock, H.W., & Babcock, H.D, *Astrophys. J.* 121, 349, 1955.
5. Howard, R.F., *Astrophys. J.* 130, 193, 1959.
6. Leighton, R.B., *Astrophys. J.* 130, 366, 1959.
7. Sheeley, N.R., *Sol. Phys.* 1, 171, 1967.
8. Chapman, G. A., & Sheeley, N.R., *Sol. Phys.* 5, 442, 1968.
9. Skumanich, A., et al., *Astrophys. J.* 200, 747–764, 1975.
10. Schrijver, C.J., *Astron. Astrophys.* 172, 111, 1987.
11. Schrijver, C.J., et al., *Astrophys. J.* 337, 964, 1989.
12. Harrison, R.A., et al., *Sol. Phys.* 162, 233–290, 1995.
13. Wilhelm, K., et al., *Sol. Phys.* 162, 189, 1995.
14. Thompson, W.T., *CDS Software Note* 49, 1998.
15. Haugan, S.V.H., *Sol. Phys.* 178/2, 275, 1999.
16. Pauluhn, A., et al., *ISSI Sci. Rep.* SR-002, in press, 2002.
17. Scherrer, P., et al., *Sol. Phys.* 162, 2, 1995.
18. Pauluhn, A., & Solanki, S.K., in *Proc. SOHO-11* Davos, 2002.
19. Pauluhn, A., & Solanki, S.K., in prep. 2002.
20. Simon, G.W., & Leighton, R.B., *Astrophys. J.* 140, 1120, 1964.
21. Frazier, E.N., *Sol. Phys.* 21, 42, 1971.
22. Mehltretter, J.P., *Sol. Phys.* 38, 43, 1974.
23. Cook, J.W., et al., *Astrophys. J. Lett.* 270, L89, 1983.
24. Foing, B., & Bonnet, R.M., *Astrophys. J.* 279, 848, 1984.
25. Foing, B., *Astron. Astrophys.* 162, 292, 1986.
26. Cook, J.W.,& Ewing, J.A., *Astrophys. J.* 355, 719, 1990.
27. Beckers, J.M., Physics of Solar Planetary Environments, 89, 1976.
28. Daras-Papamargaritis, H., & Koutchmy, S., *Astron. Astrophys.* 125, 280, 1983.
29. Spruit, H.C., & Zwaan, C., *Sol. Phys.* 70, 207, 1981.
30. Harvey, K., & White, O.R., *Astrophys. J.* 515, 812–831, 1999.
31. Solanki, S.K., et al., *Astron. Astrophys.* 250, 230, 1991.
32. Schrijver, C.J., *Astron. Astrophys.* 269, 395, 1993.
33. Carlsson, M., & Stein, R.F., *Astrophys. J. Lett.* 440, L29, 1995.
34. Rabin, D., & Dowdy, J.F., *Astrophys. J.* , 398, 665, 1992.
35. Brković, A., et al., *Astron. Astrophys.* 353, 1083, 2000.
36. Brković, A., et al., *Astron. Astrophys.* 385, 257, 2002.